Speciation of Human Plasma High-Density Lipoprotein (HDL): HDL Stability and Apolipoprotein A-I Partitioning†

Henry J. Pownall,* Brian D. Hosken, Baiba K. Gillard, Catherine L. Higgins, Hu Yu Lin, and John B. Massey

Section of Atherosclerosis and Vascular Medicine, Department of Medicine, Baylor College of Medicine, Houston, Texas 77030

Received March 13, 2007; Revised Manuscript Received April 24, 2007

ABSTRACT: The distribution of apolipoprotein (apo) A-I between human high-density lipoproteins (HDL) and water is an important component of reverse cholesterol transport and the atheroprotective effects of HDL. Chaotropic perturbation (CP) with guanidinium chloride (Gdm-Cl) reveals HDL instability by inducing the unfolding and transfer of apo A-I but not apo A-II into the aqueous phase while forming larger apo A-I deficient HDL-like particles and small amounts of cholesteryl ester-rich microemulsions (CERMs). Our kinetic and hydrodynamic studies of the CP of HDL species separated according to size and density show that (1) CP mediated an increase in HDL size, which involves quasi-fusion of surface and core lipids, and release of lipid-free apo A-I (these processes correlate linearly), (2) >94% of the HDL lipids remain with an apo A-I deficient particle, (3) apo A-II remains associated with a very stable HDL-like particle even at high levels of Gdm-Cl, and (4) apo A-I unfolding and transfer from HDL to water vary among HDL subfractions with the larger and more buoyant species exhibiting greater stability. Our data indicate that apo A-I's on small HDL (HDL-S) are highly dynamic and, relative to apo A-I on the larger more mature HDL, partition more readily into the aqueous phase, where they initiate the formation of new HDL species. Our data suggest that the greater instability of HDL-S generates free apo A-I and an apo A-I deficient HDL-S that readily fuses with the more stable HDL-L. Thus, the presence of HDL-L drives the CP remodeling of HDL to an equilibrium with even larger HDL-L and more lipid-free apo A-I than with either HDL-L or HDL-S alone. Moreover, according to dilution studies of HDL in 3 M Gdm-Cl, CP of HDL fits a model of apo A-I partitioning between HDL phospholipids and water that is controlled by the principal of opposing forces. These findings suggest that the size and relative amount of HDL lipid determine the HDL stability and the fraction of apo A-I that partitions into the aqueous phase where it is destined for interaction with ABCA1 transporters, thereby initiating reverse cholesterol transport or, alternatively, renal clearance.

Human plasma high-density lipoprotein cholesterol concentration (HDL-C) is negatively correlated with the incidence of cardiovascular disease (CVD) (*1*, *2*). Although this correlation is not perfect, increasing HDL-C in a way that is cardioprotective remains an important public health goal (*3*). The putative protective mechanism underlying this correlation is reverse cholesterol transport (RCT), a process by which cholesterol in peripheral tissue is transferred via HDL[1] to the liver for recycling or catabolism (*4*). Cholesterol efflux is mediated by ATP-binding cassette transporter (ABC) G1, which is strongly expressed in macrophages (*5*−*7*), reversible spontaneous cholesterol desorption from the plasma membrane into the surrounding aqueous phase (*8*−*10*), and efflux via SR-B1, which also mediates selective hepatic uptake of HDL lipids (*11*); these mechanisms require phospholipid in the acceptor. Interaction of lipid free apolipoproteins (apos) with the ABCA1 transporter also triggers the efflux of cholesterol and PC as early forms of HDL (*12*−*14*). Tangier disease, a low-plasma HDL state, is due to transport-incompetent variants of ABCA1 (*15*, *16*).

The relative importance of HDL versus lipid-free apo A-I in RCT remains unresolved. On one hand, apo A-I, which is the most abundant apo that elicits cholesterol efflux via ABCA1, triggers efflux only as the lipid-free protein, and nearly all apo A-I is associated with HDL. On the other hand, efflux via SR-BI and ABCG1 to HDL is a function of its PC content, the cholesterol-binding component of HDL; this correlation might underlie the negative correlation between plasma HDL-C and CVD (*6*, *17*−*22*). Nevertheless, the role of free apos and their target for cellular cholesterol efflux, ABCA1, cannot be discounted because numerous human variants of ABCA1 are associated with low HDL-C (*15*, *16*).

HDL comprises cholesterol, cholesteryl esters, phospholipids, small amounts of triglyceride, and apos that include apos A-I, A-II, C, and E. Whereas transfer of apos from the lipid-bound form to the lipid-free form is required for ABCA1 transport, the stability of HDL depends on a nontransferrable component that remains associated with

† Supported by grants in aid from the National Institutes of Health (HL-30914, HL-56865, and HL07812).

* To whom correspondence should be addressed: Baylor College of Medicine, One Baylor Plaza, MS A601, Houston, TX 77030. Phone: (713)798-4160. Fax: (713)798-9005. E-mail: hpownall@bcm.tmc.edu.

[1] Abbreviations: apo, apolipoprotein; CP, chaotropic perturbation; CERM, cholesteryl ester-rich microemulsion; HDL and LDL, high- and low-density lipoprotein(s), respectively; FC, free cholesterol; CE, cholesteryl ester; PL, phospholipid; PC, phosphatidylcholine; PO, 1-palmitoyl-2-oleoyl; SPD, 1-stearoyl-2-pyrenedecanoyl; Gdm-Cl, guanidinium chloride; SEC, size exclusion chromatography; TBS, Tris-buffered saline.

10.1021/bi700496w CCC: $37.00
Published on Web 05/27/2007

HDL. Herein, we use CP and size exclusion chromatography (SEC) to show that HDL particle size is a determinant of HDL stability, CP-induced HDL fusion is not a simple binary process, and the CP-induced distribution of apo A-I between HDL and water is a simple partitioning reaction that is governed by the relative amounts of HDL and water. Unlike other methods, SEC permits chemical analysis of the CP products, which supports more substanitve conclusions about the physiochemical basis of HDL stability.

MATERIALS AND METHODS

Materials. HDL were isolated according to density by sequential flotation of pooled human plasma obtained from The Methodist Hospital Blood Donor Center (*23*). The HDL subfractions were separated by SEC in which an increasing elution volume corresponds to a decreasing particle size; the column was calibrated using globular proteins with known Stokes radii. SEC was conducted using a pair of Pharmacia Superose HR6 columns in tandem; when required, 1 mL fractions were collected, and fractions from multiple 0.5 mL injections were pooled and concentrated as needed by placing the sample in a dialysis sack (12000−14000 MW exclusion) and placing Sephedex G75 on the outside to remove water. Alternatively, HDL (330 mg) was separated into 10 fractions by ultracentrifugation in a density gradient between 1.11 and 1.17 g/mL created with KBr. Four fractions [HDL_2 and buoyant (B), intermediate (I), and dense (D) HDL_3 with densities of 1.11, 1.13, 1.15, and 1.17 g/mL, respectively (HDL_3-B, HDL_3-I, and HDL_3-D)] were selected for further testing by CP. These fractions contained ~5, 8, 15, and 6% of the total HDL protein, respectively. Apolipoprotein compositions were determined by SDS−PAGE using 15% Tris-Glycine Ready Gels (Bio-Rad). Bands were visualized with Pierce GelCode Blue stain reagent, destained, and recorded by photography. The apo A-I and apo A-II contents of the HDL subfractions were not remarkably different (data not shown). Ultrapure Gdm-Cl and other buffer components were from Fisher Scientific. Although other chaotropes would be expected to yield similar results, guanidinium chloride (Gdm-Cl) was used so that our data could be interpreted in the context of past reports on HDL stability from others. Stock solutions of 9 M Gdm-Cl were warmed to ~37 °C prior to use to dissolve the Gdm-Cl. All experiments were conducted in TBS [10 mM Tris, 100 mM NaCl, 1 mM EDTA, and 1 mM NaN_3 (pH 7.4)].

Labeling of HDL with [^{3}H]CE and [^{3}H]POPC. [^{3}H]-Cholesterol (0.1 mCi) was dried under vacuum and redissolved in 100 μL of 95% ethanol. HDL (2 mL, 9.6 mg/mL) was combined with the LCAT activity from the clear zone obtained from the flotation of HDL (4 mL), and the ethanolic solution of labeled lipid was added dropwise with stirring and incubated at 37 °C with mild agitation. Conversion of FC to CE was followed by removing 100 μL at various times, extracting the mixture into hexane, and assessing formation of CE by thin layer chromatography. To remove remaining unreacted FC, the HDL was mixed with LDL (5 mL, 5.8 mg/mL) and incubated for 3 h at 37 °C. At the end of the incubation, the density was adjusted to 1.063 g/mL and the LDL floated and removed. The labeled HDL was adjusted to a *d* of 1.21 g/mL by adding KBr and the [^{3}H]CE-labeled HDL (0.8 μCi/mg of protein) isolated by flotation. According to liquid scintillation counting of spots collected after thin layer chromatography, 97% of the radioactivity eluted as CE. Phospholipid label was incorporated into HDL by dispersing 50 μL of an ethanolic solution of [^{3}H]POPC into a solution of HDL followed by dialysis versus TBS. The SEC profiles of HDL protein absorbance (280 nm) coeluted with both [^{3}H]-POPC and [^{3}H]CE radioactivity.

SPDPC Labeling of HDL. The pyrene-labeled PC, SPDPC, which was synthesized and purified according to the method of Mason et al. (*24*), comigrated with a PC standard as a single fluorescent, phosphorus-positive species during thin layer chromatography over silica gel using a mobile phase of chloroform, methanol, and water (65/25/4). SPDPC (50 μL, 4.4 mM in ethanol) was dispersed into a stirred solution of HDL (1 mL; 10 mg/mL protein, 6.9 mM PL as choline) with a Hamilton syringe at ambient temperature. SPDPC represented ~3 mol % of the total HDL phospholipid.

Circular Dichroism (CD). The effects of various Gdm-Cl concentrations on the ellipticity of the HDL subfractions (50 μg of protein/mL) were determined after incubation at room temperature for 24 h. Ellipticities were recorded on a Jasco 810 spectropolarimeter (2 mm path), and the results were plotted in terms of the percent of total change in ellipticity versus Gdm-Cl concentration.

SEC. Effects of CP on HDL were determined by mixing Gdm-Cl with HDL under various conditions of temperature, concentration, and incubation time. HDL and their subfractions were combined with TBS and 9 M Gdm-Cl at ambient temperatures to give final protein concentrations of 0.5−1.0 mg/mL and final Gdm-Cl concentrations from 0 and 6 M. After being mixed and incubated for various times, aliquots were analyzed by SEC using an Amersham-Pharmacia ÄKTA chromatography system equipped with two Superose HR6 columns in tandem. Typically, the sample was filtered (0.2 μm), and 0.2 mL was injected into the chromatograph and eluted with TBS. Column effluent was monitored by absorbance at 280 nm and the radioactivity of collected fractions. Stokes radii for the fractions were calculated from a calibration curve using protein standards of known size. Particle volumes (*V*) were calculated using the relation $V = {}^4/_3\pi r^3$. For preparative chromatography, a 0.5 mL sample loop was used and fractions from multiple runs were sometimes pooled and analyzed.

Analysis of CP of HDL by SEC. CP data plotted as %LFA versus Gdm-Cl concentration were fitted to a four-parameter sigmoidal curve, where $\%LFA = \%LFA_0 + \%LFA_{max}/\{1 + \exp-[([\text{Gdm-Cl}] - [\text{Gdm-Cl}]_0)/b]\}$, where %LFA is the percent lipid-free apo A-I, [Gdm-Cl] is the molar concentration of Gdm-Cl, $[\text{Gdm-Cl}]_0$ is the Gdm-Cl concentration at the midpoint of the curve, $\%LFA_{max}$ is the maximum value for the %LFA, and *b* is a parameter representing transition cooperativity, with a smaller value representing a sharper (more cooperative) transition. To determine the effect of HDL concentration on stability to CP, HDL was serially diluted in 3 M Gdm-Cl, incubated for 68 ± 4 h at room temperature, and analyzed by SEC. The proportion of free to lipid-bound apo A-I was plotted as a function of HDL-PL concentration.

Kinetics. The kinetics of CP-induced remodeling of HDL by Gdm-Cl were measured by SEC and the excimer fluorescence of SPDPC. The kinetics of apo A-I release were measured by monitoring the rate of appearance of lipid-free

apo A-I by SEC. HDL (1 mg/mL) and 3 M Gdm-Cl were combined at room temperature and aliquots removed at various times and analyzed by SEC. Kinetics were based on the rate of appearance of the integrated absorbance of apo A-I (see the legend of Figure 1 for other details). The kinetics of HDL fusion were also measured in real time by monitoring the disappearance of pyrene excimer fluorescence following the mixing of SPDPC-labeled (~3% total phospholipid) and unlabeled HDL. Labeled and unlabeled HDL were mixed in the same concentrations used to study the release of apo A-I by SEC, i.e., 1 mg/mL HDL protein. All reagents were preincubated at the experimental temperature before the fusion reaction was initiated. Labeled HDL (10 μL, 10 mg/mL), unlabeled HDL (90 μL, 10 mg/mL), and various ratios of TBS and Gdm-Cl were mixed in order in fluorescence cuvettes to achieve final Gdm-Cl concentrations between 0 and 4.8 M. Activation energies (E_a) were calculated from the temperature dependence of the rate constant according to the relation $k = A \exp(-E_a/RT)$; the slope of the line obtained from the first-order linear regression analysis of ln k versus $1/T$ is $-E_a/R$.

RESULTS

Kinetics of CP of HDL. The kinetics of CP of HDL were followed by SEC and the excimer fluorescence of pyrenyl lipids, which are real time sensors for the mixing of HDL surface components (*31*). The respective appearance and disappearance of absorbance corresponding to free apo A-I and HDL were slow enough to follow by SEC (Figure 1A). At 24 °C, the respective first-order rate constants for the appearance of free apo A-I and the disappearance HDL were similar (0.190 ± 0.03 and -0.193 ± 0.04 h^{-1}, respectively). The respective activation energies calculated from the slopes of Arrhenius plots (Figure 1, insets) were 113 ± 8 and 110 ± 4 kJ/mol. The respective enthalpy and entropy of formation of the activated state were calculated as follows: $\Delta H^{\ddagger} = E_a - RT = 107.5 \pm 8$ kJ and $\Delta S^{\ddagger} = 2.303R \log NhX/RT = 38.9 \pm 6$ J/EK, where R is the gas constant, T is the absolute temperature, k is the reaction rate constant, N is Avogadro's number, h is Planck's constant, and $X = k/(\exp -\Delta H/RT)$. The calculated free energy of activation was as follows: $\Delta G^{\ddagger} = H^{\ddagger} - T\Delta S^{\ddagger} = 95.9$ kJ. The kinetics of HDL fusion as assessed by the pyrene excimer assay of Lusa et al. (*26*) gave a rate constant for fusion that increased with an increasing Gdm-Cl concentration: $k = 0.057 \pm 0.004$, 0.103 ± 0.004, and 0.153 ± 0.009 h^{-1} at 3, 4, and 5 M Gdm-Cl, respectively (Figure 2). These data complement the SEC data of Figure 1 by revealing the CP-mediated fusion of the polar lipid components of HDL with rate constants that are similar to those for the appearance of larger HDL-like particles and the release of apo A-I.

Effect of CP on HDL Species Separated by Size. Because CP appears to effect formation of larger HDL particles, we examined CP-mediated changes in HDL species separated according to size. HDL was separated by SEC and analyzed 24 h and 6 days after being mixed with various final Gdm-Cl concentrations. Four size fractions were collected (Figure 3A, inset) and analyzed. The SEC data show that the size fractions (1−4) correspond to distinct profiles in which the respective decreasing peak elution volumes correspond to increasing size (Figure 3A−H, shaded curves). With the addition of increasing Gdm-Cl concentrations, the

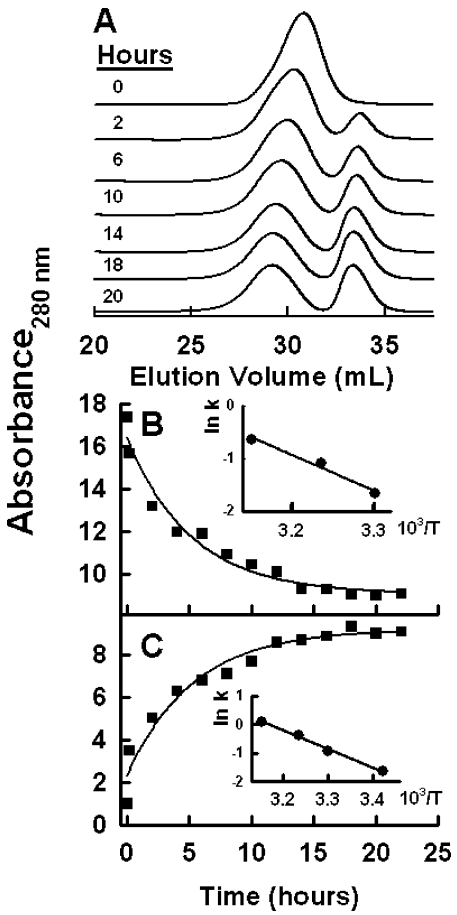

FIGURE 1: Kinetics of CP of HDL as assessed by SEC. (A) Representative SEC profiles of HDL (1 mg/mL) following incubation with 3 M Gdm-Cl; incubation times are given at the left of each panel. (B and C) Kinetics of CP according to the respective rates of disappearance and appearance of the peaks of absorbance corresponding to HDL (29−31 mL) and free apo A-I (32−36 mL) in the SEC profile. The respective first-order rate constants at 24 °C, calculated from a fit to the data in panels B and C, were −0.190 and 0.193 h^{-1}, respectively. From the temperature dependence of the respective rates of disappearance of HDL and appearance, apo A-I activation energies of 113 ± 8 and 110 ± 4 kJ/mol were determined from Arrhenius plots (B and C, respectively).

magnitudes of the peaks at ~15 and ~34 mL increase, with the latter skewed to a smaller elution volume that corresponds to a larger species. Concurrently, the major shaded HDL peak gradually shifts to earlier elution volumes, indicating an increase in HDL particle size with release of apo A-I. A previous study (*27*) and data below show that the 34 mL peak contains apo A-I and no detectable apo A-II. Experiments in which the apo A-I concentration was varied showed a shift in the peak for lipid-free apo A-I; from this, we conclude that the peak shift of the released apo A-I in our SEC experiments is due to self-association, which is expected with an increase in apo A-I concentration (data not shown). One difference among the elution profiles of the variously sized HDL species was the decrease in the magnitude of the peak appearing in the void volume with decreasing particle size. Qualitatively, data collected at 24 h and 6 days were similar (panels A−D and E−H of Figure 3, respectively), consistent with half-times calculated from Figure 1.

Effect of CP on HDL Apos. SDS−PAGE revealed, as expected, that the major proteins in HDL are apos A-I and A-II (Figure 4A,D, lane a). On the basis of its elution volume

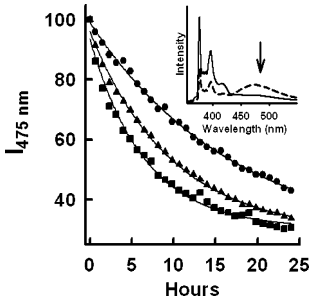

FIGURE 2: Kinetics of HDL fusion as assessed by the disappearance of SPDPC excimer fluorescence. The inset shows the fluorescence of HDL containing SPDPC before (- - -) and 36 h after (—) mixing unlabeled HDL and SPDPC-labeled HDL. Curves correspond to the time dependence of the excimer fluorescence (475 nm) of SPDPC following mixing of labeled and unlabeled HDL and incubation in 3 (●), 4 (▲), and 5 M Gdm-Cl (■) for 36 h at 24 °C. The lines are three-parameter exponential fits of the data according to the relation $I_t = I_0 + ae^{-kt}$, where I_t and I_0 are the excimer fluorescence intensities at time t and at the start ($t = 0$) of the reaction, respectively, a is a pre-exponential factor, and k is the rate constant; $k = 0.057 \pm 0.002$, 0.103 ± 0.002, and 0.153 ± 0.004 h^{-1} at 3, 4, and 5 M Gdm-Cl, respectively.

(34 mL), and SDS−PAGE analysis (Figure 4D), CP of HDL induced the nearly exclusive transfer of apo A-I but not apo A-II from HDL to the lipid-free form, an effect that was dose-dependent with respect to Gdm-Cl (Figure 4A−C). Concurrently, with increasing Gdm-Cl concentrations, the early eluting peak became increasingly apo A-II-rich to the extent that at 5.5 M Gdm-Cl, apo A-II was the major protein (Figure 4D, lanes b and d).

Effect of CP on HDL CE and PC. The effects of CP on the lipid components of HDL were evaluated using HDL labeled with [^{3}H]POPC and [^{3}H]CE. According to SEC, HDL was not altered by the radiolabeling procedures; protein elution profiles for [^{3}H]POPC and [^{3}H]CE radioactivity coincided with that of HDL protein absorbance (Figure 5A,D). CP of both [^{3}H]POPC- and [^{3}H]CE-labeled HDL produced similar shifts in the elution profiles for absorbance and radioactivity. Notably, very little radioactivity coeluted with the peak for apo A-I at ~34 mL. The coelution of lipid radioactivity and protein absorbance confirms that the early peak is an "HDL-like" lipoprotein. The SEC profile of [^{3}H]POPC-labeled HDL eluted with 3 M Gdm-Cl was similar to that determined in TBS except the peak for apo A-I eluted much earlier (Figure 3C); this peak coincided with that of an authentic sample of apo A-I and also eluted with Gdm-Cl. Small amounts of radiolabeled POPC and CE, ~6 and ~9%, respectively, were eluted in the void volume, suggesting that this is a cholesteryl ester-rich microemulsion (CERM). These data show that after CP, the majority of the HDL phospholipid and cholesteryl ester is associated with HDL-like particles while a minor amount occurrs in a CERM that elutes in the void volume, and that apo A-I is released in a lipid-free form, i.e., without PC or CE.

Dose-Dependent Effects of CP on HDL Size and Release of Apo A-I. Previous studies showed that relative to free apos, apos within HDL are more stable and require higher concentrations of chaotropic agents for unfolding (*28*−*32*). Using SEC, we compared the effects of various doses of Gdm-Cl on HDL. Between 0 and 5 M, Gdm-Cl induced a dose-dependent increase in the percent of total lipid-free apo A-I (shaded areas of profiles) that increased to ~60% at

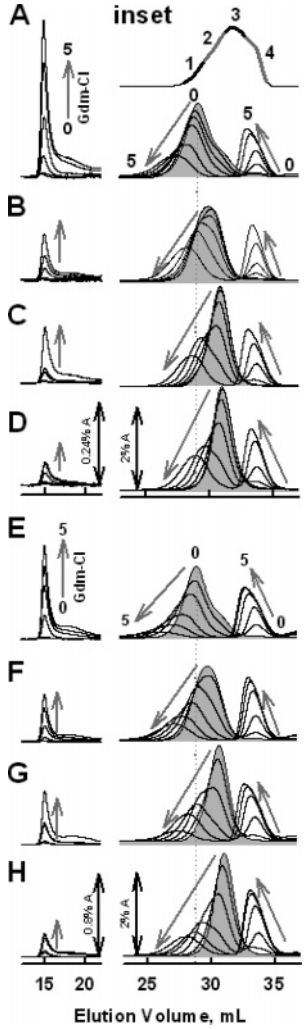

FIGURE 3: Effects of long-term CP on HDL as a function of starting HDL particle size. HDL were separated by size into fractions 1−4 (inset). Each HDL subfraction (1 mg/mL) was then incubated with Gdm-Cl at 0, 1, 2, 3, 4, or 5 M for 24 h (A−D) or 6 days (E−H) and analyzed by SEC. The shaded peak in each chromatogram corresponds to the starting (0 M Gdm-Cl) HDL, with the data for large (fraction 1) and small (fraction 4) starting HDL shown in panels A−D and E−H, respectively. Arrows show the direction of the shift in adjacent curves with increasing (0−5 M) Gdm-Cl concentrations. In panels D and H, the scales for the percent total absorbance for the early and late parts of the chromatograms are indicated for A−D and E−H, respectively. Note that the scale for the early part of panels E−H is less sensitive than that for panels A−D, reflecting the increased number of large particles in the void volume after the 6 day incubation. The vertical dotted line through panels A−D and E−H shows the midpoint of the starting HDL subfraction 1 compared to the other starting (shaded) subfractions (2, 3, and 4), and to the products after CP.

5 M Gdm-Cl (Figure 6A,C). Concurrently, the particle volumes corresponding to the peak HDL fraction were 620, 650, 730, 840, 1000, and 1100 nm^3 as the Gdm-Cl concentration increased from 0 to 1, 2, 3, 4, and 5 M, respectively; between 0 and 5 M Gdm-Cl, the particle volume of the HDL fraction increased to 177% of its original size (Figure 6C). Thus, rather than a bimodal distibution of the early eluting peak that would represent the simple conversion of native HDL to a binary fusion product, there was a gradual shift in the peak volume with each molar increment of Gdm-Cl concentration. The increase in the percent of lipid-free apo A-I and the change in the volume of HDL with an increase

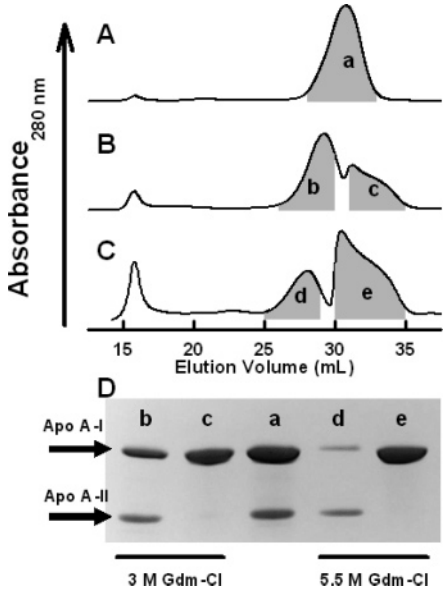

FIGURE 4: Protein composition of HDL before and after CP: (A) starting HDL (1 mg/mL) and (B and C) HDL after CP for 24 h at 24 °C in 3 and 5.5 M Gdm-Cl, respectively. (D) SDS−PAGE (15%) of HDL before and after CP. SEC fractions were pooled as indicated by shaded regions a−e in the chromatograms In panels A−C, the lanes containing the factions are labeled accordingly. Note that released lipid-free protein fractions c and e contain apo A-I but not apo A-II (lanes c and e, respectively), and the ratio of apo A-I to apo A-II is decreased in the CP-remodeled HDL product (lanes b and d) compared to that in the starting HDL (lane a).

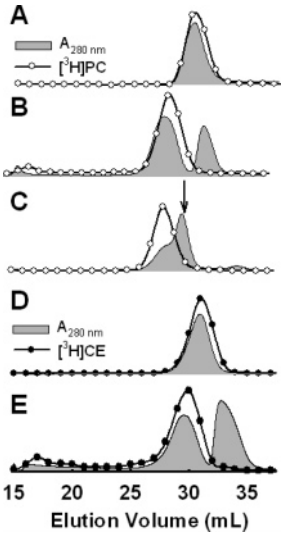

FIGURE 5: Effect of CP on the distribution of lipid-bound HDL. SEC profiles of HDL−[^{3}H]PC and HDL−[^{3}H]CE were determined before and after incubation with 3 M Gdm-Cl for 24 h. HDL−[^{3}H]PC before (A) and after (B and C) CP (○) and HDL−[^{3}H]CE before (C) and after (D) CP (●). Absorbance at 280 nm (shaded area). The eluting solvent was TBS for panels A, B, D, and E or 3 M Gdm-Cl for panel C; the arrow in panel C marks the elution volume for an authentic sample of apo A-I in 3 M Gdm-Cl.

in Gdm-Cl concentration were linearly correlated [$r^2 > 0.99$ (Figure 6D)]. The effects of Gdm-Cl were irreversible; the SEC profile after CP and removal of Gdm-Cl by dialysis were nearly identical to that obtained without dialysis (Figure 6B). The HDL peak widths at half-height were nearly the same (2.62 ± 0.05 mL; range of 2.43−2.74 mL) at all Gdm-Cl concentrations and were only slightly different when converted to molecular volume (521 ± 48 nm^3; range of

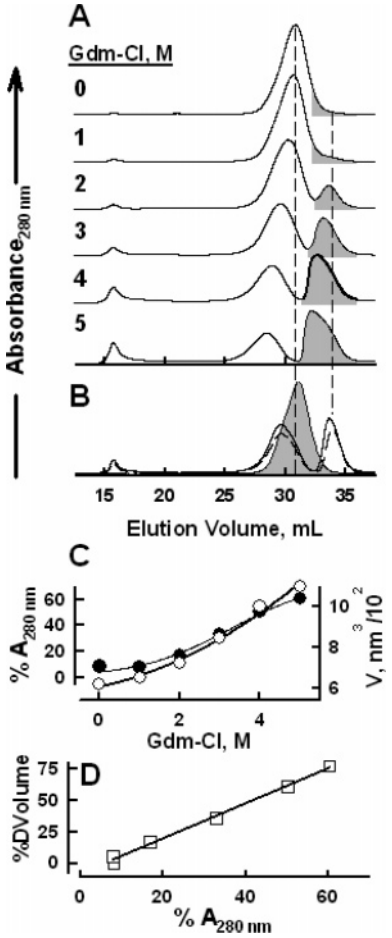

FIGURE 6: Increase in HDL particle size correlates with release of apo A-I upon CP of HDL. (A) SEC of HDL as a function of Gdm-Cl concentration. Gdm-Cl concentrations are given at the left of each panel. Gdm-Cl was incubated with HDL (1 mg/mL protein) for 24 h at 24 °C, after which each sample was analyzed by SEC. (B) Irreversibility of chaotropic perturbation (CP): HDL before (shaded area) and after CP (−) and after CP and dialysis (- - -). (C) Plot of percent absorbance [%A_{280} (●)] within the shaded areas of the traces in panel A, corresponding to released lipid-free apo A-I, vs the concentration of Gdm-Cl. A fit of the data to the equation $A_{280} = a/[1 + \exp -(C/b)]$, where a and b are constants and C is the concentration of Gdm-Cl, which gives an a of 74 ± 9 and a b of 1.13 ± 0.2; plot of the volume of the HDL fusion particle [V, mm^3/10^2 (○)] vs the concentration of Gdm-Cl that produced it. Particle volumes were calculated on the basis of the peak elution volume and a calibration curve using proteins with known Stokes diameters; volume was calculated as $V = {}^4/_3 r^3$. (D) Correlation of the percent increase in particle volume (%V) with the percent increase in lipid-free apo A-I.

419−701 nm^3). The small dose-dependent increase in absorbance that appears in the void volume likely corresponds to the large fusion particles previously observed by electron microscopy (*28*). Thus, Gdm-Cl-induced release of apo A-I and increased mean HDL particle size are highly correlated.

CP of HDL Species Separated by Density. Human HDL is bimodally distributed into two distinct density ranges that have been designated as HDL_2 ($d = 1.063-1.125$ g/mL) and HDL_3 ($d = 1.125-1.21$ g/mL). Moreover, numerous clinical studies of HDL have shown different distributions of HDL_2 and HDL_3 according to differing genetic backgrounds and therapeutic interventions. The well-known effects of Gdm-Cl on the circular dichroism spectrum of HDL (*28*, *29*) were

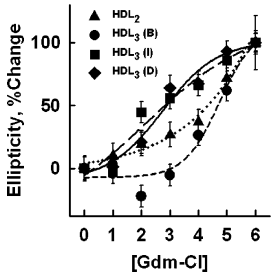

FIGURE 7: Analysis of the CP of HDL density subfractions asssessed by circular dichroism. Densities of HDL subfractions are as follows: $d(HDL_2) < 1.11$ g/mL, $d(HDL_3\text{-B}) = 1.13$ g/mL, $d(HDL_3\text{-I}) = 1.15$ g/mL, and $d(HDL_3\text{-D}) > 1.17$ g/mL. See Materials and Methods for details of the fractionation.

used to assess the differential effects of CP on HDL_2 and three HDL_3 density subfractions, HDL_3-B, HDL_3-I, and HDL_3-D (see Materials and Methods). As expected, increased amounts of Gdm-Cl reduced the molar ellipticity of all four lipoprotein species (data not shown). Expressed in terms of the percent change in ellipticity, distinct differences among the HDL species could be discerned. The Gdm-Cl dose required to reach 50% of the total change in ellipticity increased in the following order: HDL_3-I ~ HDL_3-D < HDL_2 < HDL_3-B (Figure 7). Thus, according to this measure of ellipticity, the larger, more buoyant HDL particles are more stable to CP than are the small, dense ones.

The effect of Gdm-Cl on various HDL density subfractions was further investigated by SEC, which revealed profound differences in the total amount of HDL-bound apo A-I that was converted to lipid-free apo A-I at the maximum Gdm-Cl concentration (6 M) and the Gdm-Cl concentration corresponding to the midpoint of the titration (Figures 8 and 9 and Table 1). The midpoint values increased in the following order: HDL_3-D < HDL_3-I < HDL_2 < HDL_3-B. Whereas the slopes (b) at the midpoints of the curves for HDL_3 subspecies were similar ($b = 0.76-84$), the slope for HDL_2 was much steeper ($b = 0.55$). The parameters for total HDL were similar to those for HDL_3-I, the most abundant species (Table 1). The stability of the HDL-like particle formed by 6 M Gdm-Cl was similarly tested. HDL (1 mg/mL) was incubated with 6 M Gdm-Cl for 24 h and the SEC-isolated HDL-like product titrated with 0−6 M Gdm-Cl. Unlike native HDL, 1−6 M Gdm-Cl released very ltle lipid-free apo A-I (Figure 9). Thus, the HDL-like product of the 6 M Gdm-Cl treatment is much more stable than native HDL.

CP of Mixed HDL Subspecies. The data clearly demonstrate that CP of HDL effects release of apo A-I and formation of larger, less dense (lower percent protein) HDL particles. To probe the mechanism for the expanding HDL size, we compared the effects of CP on large (L) and small (S) HDL subfractions, isolated from total HDL by SEC as in Figure 3, labeled with [^{3}H]CE, which were combined in the presence and absence of 3 M Gdm-Cl, incubated for 20 ± 0.5 h, and analyzed by SEC. HDL-L and HDL-S exhibited distinctive SEC profiles for absorbance, and when they were mixed in the absence of Gdm-Cl, the resulting profile was essentially a superposition of those for HDL-L and HDL-S (Figure 10A). CP of HDL-L and HDL-S gave the expected shift in the elution profiles to volumes corresponding to larger particles; however, the SEC profiles of L + S following incubation in 3 M Gdm-Cl were not a superposition of CP-modified HDL-L and HDL-S

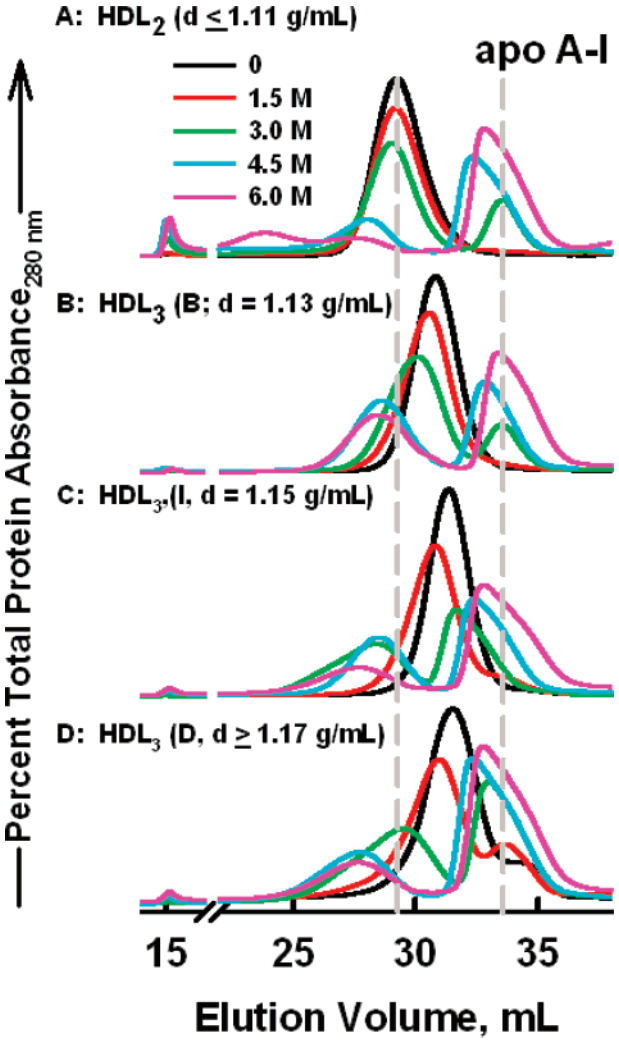

FIGURE 8: CP of HDL density subfractions assessed by SEC. HDL subfraction densities are indicated in each panel. The legend in panel A gives the chromatogram color code for the Gdm-Cl concentrations that were tested (from 0 to 6 M). The incubation time prior to SEC was 24 h.

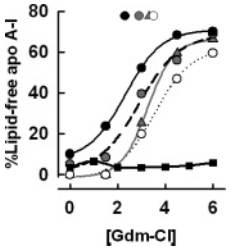

FIGURE 9: CP release of apo A-I from HDL density subfractions. The extent of apo A-I release was calculated from the data in Figure 8 and plotted as a function of Gdm-Cl concentration: (gray triangles) HDL_2, (white circles) HDL_3-B, (gray circles) HDL_3-I, and (black circles) HDL_3-D. Symbols at the top of the graph compare the respective values for the midpoints, $[GdmCl]_0$. Data were fit to a sigmoidal curve, and the parameters are given in Table 1. CP-induced release of apo A-I from HDL-like particles (black squares).

(Figure 10B). A plot of the difference between the elution profile of L + S and the numeric sum of the profiles for L and S measured separately shows little difference (Figure 10C, gray curve). In contrast, a similar plot of L, S, and L + S after CP reveals that CP of L + S forms more of the large HDL, which elutes earlier, i.e., is larger, with less of

Table 1: Parameters for the CP-Mediated Desorption of Apo A-I from HDL

HDL [*d* (g/mL)]	%LFA$_{max}$[a,b]	*b*[a,c]	[GdmCl]$_0$
total	65 ± 4	0.75 ± 0.14	3.0 ± 0.1
HDL$_2$ (≤1.11)	67 ± 3	0.55 ± 0.10	3.3 ± 0.1
HDL$_3$-B (1.13)	64 ± 6	0.76 ± 0.18	3.5 ± 0.2
HDL$_3$-I (1.15)	67 ± 15	0.84 ± 0.48	2.9 ± 0.4
HDL$_3$-D (≥1.17)	64 ± 2	0.76 ± 0.06	2.3 ± 0.1

[a] Calculated from a sigmoidal fit to data in Figure 9. [b] Calculated percent total lipid-free apo A-I as the Gdm-Cl concentration approaches infinity. [c] *b* reflects cooperativity; smaller values indicate a sharper, more cooperative transition.

the intermediate-sized HDL, and more lipid-free apo A-I [elution volumes of ∼28.5, 30.5, and 33.5 mL, respectively (Figure 10C, black curve)]. The effects of CP on the elution profiles of [^{3}H]CE-bound HDL were nearly identical except for the expected absence of peaks for lipid-free apo A-I (Figure 10D−F). Given that the final HDL product from HDL−(L + S) is larger than either HDL-L or HDL-S alone, the difference is likely due to a greater contribution of HDL-S to both increased apo A-I and more HDL-L. Thus, the presence of HDL-L potentiates the instability of HDL-S. Our data suggest that the greater instablity of HDL-S generates free apo A-I and an apo A-I-deficient HDL-S that readily fuses with the more stable HDL-L and that the presence of HDL-L drives the CP remodeling of the HDL to an equilibrium with even larger HDL-L and more lipid-free apo A-I than with either HDL-L or HDL-S alone.

Partitioning of Apo A-I between HDL and Water. The transfer of apo A-I from HDL to the aqueous phase by CP suggested that our data might be explained in part on the basis of a simple partitioning model in which apo A-I is distributed between the HDL−phospholipd (PL) surface and water according to the relative sizes of the lipid and aqueous compartments. SEC analysis of CP as a function of HDL concentration (24 h, 24 °C) at a constant Gdm-Cl concentration (3 M) showed that as the HDL concentration was reduced, an increasing fraction of HDL-bound apo A-I was transferred to the aqueous phase as lipid-free protein (Figure 11A). According to the number of molecules of free apo A-I in water (*F*) and bound to HDL (*B*), the attendant partition constant K_P is given by the equation $K_P = B[W]/F[PL]$, where [W] and [PL] are the molarities of water and phospholipid, respectively. Incorporating the molarity of water into the partition coefficient and rearranging gives the relation $F/B = K_P'/[PL]$. *F*/*B* was calculated as the ratio of the integrated absorbances measured at elution volumes between 32 and 36 mL (free apo A-I) to those between 26 and 32 mL (PL-bound apo A-I). Regression analysis of a plot of *F*/*B* versus [HDL−PL] (Figure 11B) gave the following: $F_0/B_0 = 0.67 \pm 0.08$ and $K_P' = 0.024 \pm 0.002$ mM.

DISCUSSION

CP of human HDL transfers apo A-I to water with the concomitant formation of a HDL-like particle (*28*−*33*). As reviewed by Gursky, HDL is stabilized by kinetic factors. The hallmarks of detergent perturbation (*27*) and CP (*29*), release of apo A-I and fusion of remnant HDL, emulate some of the effects of lipid transfer proteins, lecithin:cholesterol acyltransferase, and serum opacity factor (*26*, *34*−*37*). Given the distribution of HDL into subfractions with distinct structures and metabolisms, our CP studies of HDL subspecies provide insights into the mechanisms of their distinct modifications in vivo.

Kinetics and Mechanism of the CP of HDL. The kinetics of CP of HDL assessed by pyrene excimer fluorescence and SEC gave similar rate constants for the fusion of a surface component, SPDPC, and for the formation of larger HDL particles. These values are similar to each other and to those reported by Mehta et al. (*29*), whose analysis was based on time-dependent changes in protein conformation. Although there are additional small CP-induced changes at 6 days (Figure 3A,B), the reaction is essentially complete within 24 h (Figures 1 and 2), the time interval for most of our studies. Our data confirm and extend previous findings on CP-induced compositional changes (*28*−*33*). Even at 5.5 M Gdm-Cl, only apo A-I is released by CP, leaving a particle that is apo A-II-enriched, i.e., more apo A-II than apo A-I (Figure 4). Concurrent with the CP-induced changes in the HDL-apo content, we report for the first time that the HDL-like particle contains nearly all the CE and PL and that apo A-I is released without CE, PL, or apo A-II (Figures 4 and 5).

The CP-induced changes in HDL are irreversible (Figure 6B). Two factors contribute to this. One is the intrinsic instability of HDL. The other is the energy barrier for the reverse reaction. The free energy of activation associated with the formation of the activated state is 95.9 kJ; the magnitude of this barrier would be much higher for the reverse reaction, which begins at a lower free energy state (*28*, *29*). Interestingly, the majority of the free energy of activation is derived from a very high enthalpy of activation. The source of this cannot be established with certainty, but one interpretation is that in passing to the activated state, some of the hydrophobic components of HDL are transferred to water where they form a cavity in which the strong associations between water molecules are disrupted. Candidate molecules include the neutral lipids, CE and TG, or PL acyl chains. None of these seems likely because of their poor solubility in Gdm-Cl. More likely, passage to the activated state involves the exposure of the hydrophobic amino acid residues of apos to the aqueous phase, and given that only apo A-I is lost during CP, release of this apo from the lipid surface into the aqueous environment seems to be the likely source of the high enthalpic contribution to the free energy of activation. The linear correlation between the increase in the size of the HDL-like particle and the amount of apo A-I released (Figure 6C,D) suggests that these two processes are mechanistically linked.

These data support a model of HDL CP in which the intiating event is the transfer of apo A-I from HDL to the aqueous phase (Figure 12). This first step creates vacancies on the surface of HDL that expose the neutral lipid core to water. Fusion then follows by contact at vacancy sites where the neutral lipids of HDL particles coalesce, thereby creating a new larger particle. The mechanism is likely more complicated since this model would lead to a bimodal distribution of HDL particle sizes between the starting HDL and the fusion product. However, this is not observed, and only at the highest Gdm-Cl concentration is the fused HDL particle weight equal to the sum of two HDL particles less the mass of the lost apo A-I. Instead, a gradual increase in

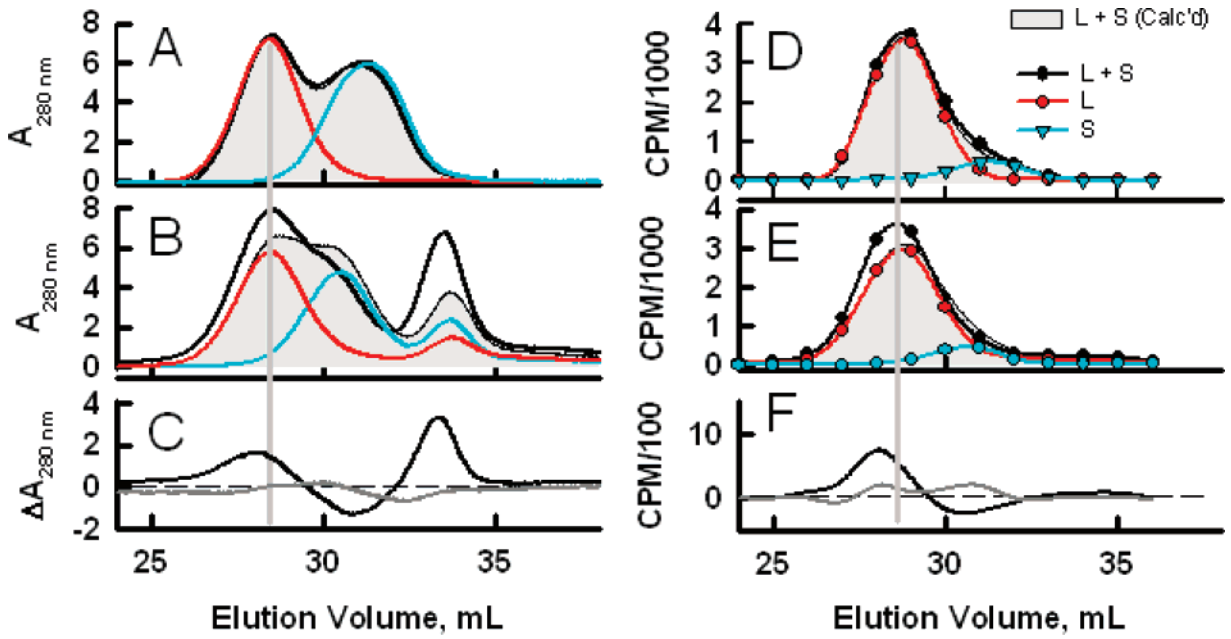

FIGURE 10: CP of mixed HDL subspecies. Large (L) and small (S) HDL subfractions were isolated by SEC, labeled with [^{3}H]CE, and treated separately or combined in the absence (A and D) or presence (B and E) of 3 M Gdm-Cl for 20 ± 0.5 h and analyzed by SEC. The left portions of panels A−C show A_{280} data and the right portions [^{3}H]CE data. (A and C) SEC profiles in control samples (0 M Gdm-Cl): HDL-L (red), HDL-S (blue), and HDL-L+S (black), mixed in a 1:1 protein ratio. The calculated sum of HDL-L plus HDL-S is shown by the shaded area. (B and E) SEC profiles after 3 M Gdm-Cl incubation, with the legend as in panels A and D. (C and F) Plots of the difference between the elution profile of HDL-(L + S) and the numeric sum of the profiles for HDL-L and HDL-S measured separately show little difference in the absence of CP (gray curve). In contrast, the difference plots of HDL-L, HDL-S, and HDL-(L + S) after CP (black curve) by both ΔA_{280} (C) and [^{3}H]CE (F) reveal an increase in the amount of large particles (elution volume of ~28 mL) and free apo A-I (elution volume of ~34 mL), with a loss of mass in the intermediate particle.

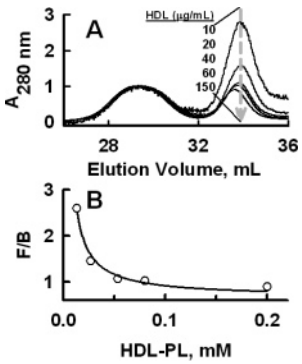

FIGURE 11: CP-mediated distribution of apo A-I between HDL and water as a function of HDL Concentration as assessed by SEC. Aliquots of HDL were combined with various volumes of 9 M Gdm-Cl and TBS to give the indicated final concentrations of protein-bound HDL and 3 M Gdm-Cl. (A) The samples were analyzed by SEC 68 ± 4 h after being mixed. The gray vertical arrow shows the direction of change with increasing HDL concentration. The profiles are normalized to the same absorbance at the elution peak for HDL. (B) The ratio of lipid-free (*F*; 32−36 mL) to lipid-bound apo A-I (*B*; 26−32 mL) is an inverse function of HDL−PL concentration. $F_0/B_0 = 0.67$; $KN_p = 0.024 \pm 0.002$ mM, and $r^2 = 0.98$.

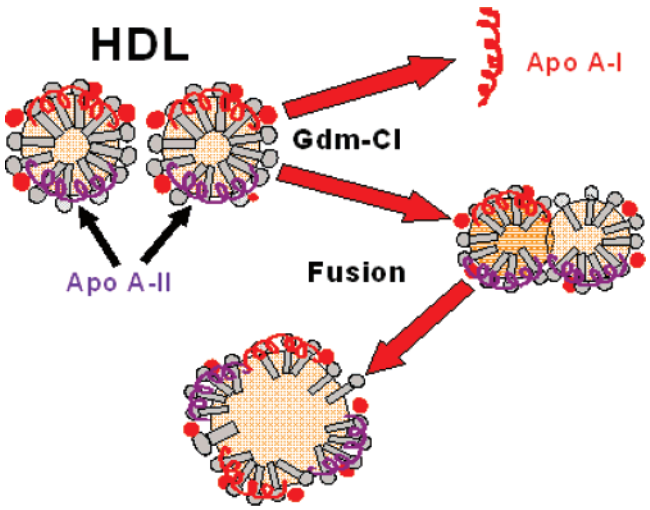

FIGURE 12: Model for the partitioning of apo A-I between HDL and water, and HDL fusion.

HDL particle weight is seen, suggesting a remodeling continuum of HDL particles during CP. Throughout this process, the ongoing transfer of apo A-I to the aqueous phase and subsequent fusion of remnant particles continues until equilibrium, a state that is characterized by large stable particles with tightly bound apo A-I and apo A-II molecules.

These changes are readily understood within the context of the principal of opposing forces as described by Tanford (*38*). In the absence of amphiphiles, CE and other neutral lipids dispersed in water tend to coalesce into a single phase. In the presence of amphiphiles, apos and phospholipids, there is a competing reaction that is driven by the hydrophobic effect, i.e., transfer of the PL acyl chains and the amino acid residues on the nonpolar face of the amphipathic helix of apo A-I to a nonpolar environment. In the various cases of starting HDL particle size or density tested here, the completion of the CP reaction is characterized by limits to the size of the HDL-like particle and the amount of lipid-free apo A-I released; the HDL compositions at these limits must correspond to the optimal thermodynamic balance for phase separation of the neutral lipids, association of all phospholipids with a particle surface, and the association of some apo A-I and all apo A-II through high-energy interac-

tions with the particle surface. The apo A-I remaining on HDL must be more lipophilic than the apo A-I that was released and may be as lipophilic as apo A-II, a conclusion that is supported by the observation that CP of the HDL-like particle does not release significant amounts of apo A-I (Figure 9). Thus, HDL contains two populations of apo A-I; one is labile and readily displaced by Gdm-Cl. The other population, like apo A-II, is strongly associated with HDL and not displaced by CP.

CP studies of rHDL containing apo A-I and PL have shown very high stability so that apo A-I is intrinsically lipophilic and like similar early forms of discoidal HDL may be quite stable. Mature spherical forms of HDL differ from rHDL through the occurrence of a neutral lipid core. Plasma HDL maturation is driven by cholesterol esterification which yields CE that are compartmentalized in the particle core. Apparently, the driving force for CE compartmentalization is great enough to form a particle that is stable with respect to CE compartmentalization but unstable with respect to apo A-I association, as revealed by CP. These changes simulate in vivo effects of phospholipid transfer protein, cholesterol ester transfer protein, and lecithin:cholesterol acyltransferase, which release apo A-I (*26*, *34*−*37*). The latter is probably most important because it forms the CE that decrease HDL particle size through the loss of the LCAT acyl donor, PC.

SEC also shows a small amount of mass eluting in the void volume (Figure 3). This fraction contains what are likely the very large particles observed in the studies of Gursky (*28*, *29*). Our data show that these contain both CE and PC (Figure 5). The amount of very large CE- and PL-rich fusion products that are observed in the void volume is relatively small and may be derived from a distinct population of the large HDL, which is CE-rich and perhaps apo A-II-poor. CP of HDL_2 forms more large particles than CP of HDL_3 (Figure 8). Although our HDL were not separated on the basis of apo A-II content, the increases in the amounts of these large particles with an increase in the size of the starting HDL (Figure 3A,E) clearly suggest that the initial size of the CE core is a determinant of the amount of very large fusion product that is formed.

CP also has some more subtle effects. As the time for CP incubation (Figure 1) and/or the Gdm-Cl concentration (Figures 1, 3, 4, 6, and 7) increases, the height of the peak for lipid-free apo A-I increases and is skewed toward higher molecular weights, both of which are positively correlated with the amount of free apo A-I. We assign this effect to apo A-I self-association, a phenomenon that has been previously reported (*39*, *40*). This is apparent under conditions where the amount of released apo A-I is ∼30% or higher. Given that the total protein loaded was 1 mg and that the apo A-I peak is distributed over 4 mL, an average concentration of self-associated apo A-I is 0.3×1 mg/4 mL $= 75$ μg/mL. Thus, this effect is likely important under pathological conditions that liberate large quantities of apos. These conditions include infections by *Streptococcus pyogenes*, which secretes a protein that rapidly opacifies mammalian plasma and liberates a large fraction of apo A-I from HDL (*37*).

Speciation of HDL Stability. Current models suggest that the number of amphipathic helical regions in apos that are associated with lipid determines the free energy of association, i.e., lipophilicity. Given that there are no known remarkable differences in the helical content of HDL subspecies, one would expect a similar lipophilicity. However, our data clearly show that the affinity of apo A-I for HDL increases with size. Apo A-I is organized into two structural domains: amino-terminal and central parts that form a helix bundle and the carboxyl-terminal "α-helices", which form a distinct quasi-organized structure (*41*, *42*). Lipid binding by apoA-I is controlled by reorganization of the helix bundle, because the rate of release of heat during binding of various apoA-I variants correlates inversely with the stability of the helix bundle. We propose that the larger surface area of HDL_3-B permits a larger number of exergonic lipid−apo interactions. In contrast, HDL_3-D has much less surface area so that not all of the potential interactions of lipid-binding α-helical segments with the HDL-PL can be satisfied. The existence and identity of these segments remain to be determined.

The behavior of HDL_2 is distinct from that of HDL_3, and despite the fact that pooled plasma was used to isolate HDL, differences among various pools of plasma from normolipidemics were not seen. In contrast, profound differences were seen in the HDL from hypertriglyceridemic patients (data not shown). The slope of the partitioning curve for HDL_2 is much steeper than that of HDL_3 and cuts accross HDL_3-I and HDL_3-B (Figure 8 and Table 1). The steepness has been attributed to a greater cooperative effect, assuming apo A-I equivalency. On the other hand and more likely, there may be a different continuum of thermodynamically distinct apo A-I species on HDL_3 and HDL_2.

Apo A-I Partitioning. Chaotropic unfolding of monomeric proteins is usually independent of protein concentration. CP of HDL is more complicated and involves protein unfolding that is revealed by changes in apo A-I helicity (*27*; Figure 7) and transfer of lipid-free apo A-I from HDL to the surrounding aqueous phase. If these two steps are concerted, the effects of CP would be independent of HDL concentration; on the other hand, if the second step involves independent partitioning of apo A-I between the HDL particle and the aqueous phase, the fraction of apo A-I transferred to water should increase with a decrease in HDL-PL concentration. Our SEC data show that as the HDL concentration is increased from 10 to 150 g of protein/mL, the amount of free protein relative to HDL-bound protein decreases (Figure 11A) and that the ratio of free to lipid-bound apo A-I increases linearly with the inverse of the HDL concentration (Figure 11B). Thus, in addition to apo A-I unfolding, CP of HDL involves partitioning of apo A-I from HDL and water. Other studies show that partitioning occurs, albeit at a much lower level, in the absence of denaturants (*43*). This effect is important because it could liberate apo A-I for interaction with the lipid transporter, ABCA1.

Distinct Physicochemical Roles of Apos A-I and A-II in Selective HDL Uptake. In the absence of large HDL, small HDL fuse to form intermediate size particles. However, in the presence of large HDL, small HDL preferentially fuse with large HDL to produce even larger particles (Figure 10). The differential effects of CP on HDL species provide a thermodynamic and mechanistic basis for HDL remodeling by the SR-BI receptor (*44*−*47*). The SR-BI receptor binds HDL and facilitates selective uptake of cholesteryl ester but not HDL protein. Analysis of plasma from genetically altered mice sheds new light on the unique place of apo A-I in HDL

catabolism (*44*). Injection of ^{125}I-labeled HDL_2 into mice overexpressing the SR-BI receptor in an apo A-I$^{-/-}$ background generates smaller HDL remnant particles that rapidly fuse with HDL; this is also observed in vitro. In the context of HDL stability, their most remarkable observation was the selective catabolism of apo A-II. Apo A-II remnants rapidly fused with plasma HDL, while apo A-I only remnants did not, leaving over time HDL remnants that were smaller and nearly devoid of apo A-II. This observation is consistent with the labile nature of apo A-I relative to apo A-II (Figure 4) and the higher lipophilicity of apo A-II so that apo A-I is removed from plasma along with the hydrophobic lipid components of HDL. CP and SR-BI unmask differences in the lipophilicities of apos A-I and A-II. Moreover, studies with CHO cells expressing SR-BI show that apo A-II-containing HDL, while not binding SR-BI as well as apo A-I-containing HDL, actually mediate more selective uptake (*47*).

HDL metabolism is complicated, and current knowledge does not permit integration of all physicochemical and cell-based studies into an internally consistent model of HDL remodeling and maturation. However, our studies shed light on the mechanisms by which HDL remodeling occurs in vivo. In particular, we demonstrate that HDL subspecies differ in their stability to perturbation, their release of apo A-I, and the ability of remnants to fuse to form larger HDL particles; CP of the HDL-like particle shows that apo A-I is intrinsically lipophilic and that native HDL contains two populations of apo A-I, one that is lipophilic and another that is labile due, perhaps, to the LCAT-mediated contraction of large, stable HDL into small, unstable HDL; last, we show that the effects of CP on HDL are more complex than those of protein unfolding and that the thermodynamics of apo A-I partitioning between HDL and the aqueous phase are also important.

REFERENCES

1. Frick, M. H., Elo, O., Haapa, K., et al. (1987) Helsinki Heart Study: Primary-prevention trial with gemfibrozil in middle-aged men with dyslipidemia. Safety of treatment, changes in risk factors, and incidence of coronary heart disease, *N. Engl. J. Med. 317* (20), 1237−1245.
2. Manninen, V., Elo, M. O., Frick, M. H., et al. (1988) Lipid alterations and decline in the incidence of coronary heart disease in the Helsinki Heart Study, *J. Am. Med. Assoc. 260*, 641−651.
3. Hamilton, J. A., and Deckelbaum, R. J. (2007) Crystal structure of CETP: New hopes for raising HDL to decrease risk of cardiovascular disease? *Nat. Struct. Mol. Biol. 14*, 95−97.
4. Fielding, C. J., and Fielding, P. E. (2001) Cellular cholesterol efflux, *Biochim. Biophys. Acta 1533*, 175−189.
5. Engel, T., Lorkowski, S., Lueken, A., Rust, S., Schluter, B., Berger, G., Cullen, P., and Assmann, G. (2001) The human ABCG4 gene is regulated by oxysterols and retinoids in monocyte-derived macrophages, *Biochem. Biophys. Res. Commun. 288*, 483−488.
6. Wang, N., Lan, D., Chen, W., Matsuura, F., and Tall, A. R. (2004) ATP-binding cassette transporters G1 and G4 mediate cellular cholesterol efflux to high-density lipoproteins, *Proc. Natl. Acad. Sci. U.S.A. 101*, 9774−9779.
7. Nakamura, K., Kennedy, M. A., Baldan, A., et al. (2004) Expression and regulation of multiple murine ATP-binding cassette transporter G1 mRNAs/isoforms that stimulate cellular cholesterol efflux to high density lipoprotein, *J. Biol. Chem. 279*, 45980−45989.
8. Phillips, M. C., Johnson, W. J., and Rothblat, G. H. (1987) Mechanisms and consequences of cellular cholesterol exchange and transfer, *Biochim. Biophys. Acta 906*, 223−276.
9. Phillips, M. C., Gillotte, K. L., Haynes, M. P., Johnson, W. J., Lund-Katz, S., and Rothblat, G. H. (1998) Mechanisms of high density lipoprotein-mediated efflux of cholesterol from cell plasma membranes, *Atherosclerosis 137* (Suppl.), S13−S17.
10. Lund-Katz, S., Laboda, H. M., McLean, L. R., and Phillips, M. C. (1988) Influence of molecular packing and phospholipid type on rates of cholesterol exchange, *Biochemistry 27*, 3416−3423.
11. Acton, S., Rigotti, A., Landschulz, K. T., Xu, S., Hobbs, H. H., and Krieger, M. (1996) Identification of scavenger receptor SR-BI as a high density lipoprotein receptor, *Science 271*, 518−520.
12. Hara, H., and Yokoyama, S. (1991) Interaction of free apolipoproteins with macrophages. Formation of high density lipoprotein-like lipoproteins and reduction of cellular cholesterol, *J. Biol. Chem. 266*, 3080−3086.
13. Bielicki, J. K., Johnson, W. J., Weinberg, R. B., Glick, J. M., and Rothblat, G. H. (1992) Efflux of lipid from fibroblasts to apolipoproteins: Dependence on elevated levels of cellular unesterified cholesterol, *J. Lipid Res. 33*, 1699−1709.
14. Yancey, P. G., Bielicki, J. K., Johnson, W. J., Lund-Katz, S., Palgunachari, M. N., Anantharamaiah, G. M., Segrest, J. P., Phillips, M. C., and Rothblat, G. H. (1995) Efflux of cellular cholesterol and phospholipid to lipid-free apolipoproteins and class A amphipathic peptides, *Biochemistry 34*, 7955−7965.
15. Okuhira, K., Tsujita, M., Yamauchi, Y., Abe-Dohmae, S., Kato, K., Handa, T., and Yokoyama, S. (2004) Potential involvement of dissociated apoA-I in the ABCA1-dependent cellular lipid release by HDL, *J. Lipid Res. 45*, 645−652.
16. Francis, G. A., Knopp, R. H., and Oram, J. F. (1995) Defective removal of cellular cholesterol and phospholipids by apolipoprotein A-I in Tangier Disease, *J. Clin. Invest. 96*, 78−87.
17. Yancey, P. G., de la Llera-Moya, M., Swarnakar, S., et al. (2000) High density lipoprotein phospholipid composition is a major determinant of the bi-directional flux and net movement of cellular free cholesterol mediated by scavenger receptor BI, *J. Biol. Chem. 275*, 36596−36604.
18. Jian, B., de la Llera-Moya, M., Royer, L., Rothblat, G., Francone, O., and Swaney, J. B. (1997) Modification of the cholesterol efflux properties of human serum by enrichment with phospholipid, *J. Lipid Res. 38*, 734−744.
19. Picardo, M., Massey, J. B., Kuhn, D. E., Gotto, A. M., Jr., Gianturco, S. H., and Pownall, H. J. (1986) Partially reassembled high density lipoproteins. Effects on cholesterol flux, synthesis, and esterification in normal human skin fibroblasts, *Arteriosclerosis 6*, 434−441.
20. Johnson, W. J., Bamberger, M. J., Latta, R. A., Rapp, P. E., Phillips, M. C., and Rothblat, G. H. (1986) The bidirectional flux of cholesterol between cells and lipoproteins. Effects of phospholipid depletion of high density lipoprotein, *J. Biol. Chem. 261*, 5766−5776.
21. Davidson, W. S., Gillotte, K. L., Lund-Katz, S., Johnson, W. J., Rothblat, G. H., and Phillips, M. C. (1995) The effect of high density lipoprotein phospholipid acyl chain composition on the efflux of cellular free cholesterol, *J. Biol. Chem. 270*, 5882−5890.
22. Gelissen, I. C., Harris, M., Rye, K. A., Quinn, C., Brown, A. J., Kockx, M., Cartland, S., Packianathan, M., Kritharides, L., and Jessup, W. (2006) ABCA1 and ABCG1 Synergize to Mediate Cholesterol Export to ApoA-I, *Arterioscler., Thromb., Vasc. Biol. 26*, 534−540.
23. Shumaker, V. N., Puppione, D. L. (1986) Sequential flotation ultracentrifugation, *Methods Enzymol. 128*, 155−169.
24. Mason, J. T., Broccoli, A. V., and Huang, C. (1981) A method for the synthesis of isomerically pure saturated mixed-chain phosphatidylcholines, *Anal. Biochem. 113*, 96−101.
25. Markwell, M. A., Haas, S. M., Bieber, L. L., and Tolbert, N. E. (1978) A modification of the Lowry procedure to simplify protein determination in membrane and lipoprotein samples, *Anal. Biochem. 87*, 206−210.
26. Lusa, S., Jauhiainen, M., Metso, J., Somerharju, P., and Ehnholm, C. (1996) The mechanism of human plasma phospholipid transfer protein-induced enlargement of high-density lipoprotein particles: Evidence for particle fusion, *Biochem. J. 313* (Part 1), 275−282.
27. Pownall, H. J. (2005) Remodeling of Human Plasma Lipoproteins by Detergent Perturbation, *Biochemistry 44*, 9714−9722.
28. Gursky, O. (2005) Apolipoprotein Stucture and Dynamics, *Curr. Opin. Lipidol. 16*, 295−300.
29. Mehta, R., Gantz, D. L., and Gursky, O. (2003) Human plasma high-density lipoproteins are stabilized by kinetic factors, *J. Mol. Biol. 328*, 183−192.

30. Reijngoud, D. J., and Phillips, M. C. (1982) Mechanism of dissociation of human apolipoprotein A-I from complexes with dimyristoylphosphatidylcholine as studied by guanidine hydrochloride denaturation, *Biochemistry 21*, 2969−2976.
31. Jayaraman, S., Gantz, D. L., and Gursky, O. (2006) Effects of salt on the thermal stability of human plasma high-density lipoprotein, *Biochemistry 45*, 4620−4628.
32. Rosseneu, M., Van Tornout, P., Lievens, M. J., Schmitz, G., and Assmann, G. (1982) Dissociation of apolipoprotein AI from apoprotein-lipid complexes and from high-density lipoproteins. A fluorescence study, *Eur. J. Biochem. 128*, 455−460.
33. Nichols, A. V., Gong, E. L., Blanche, P. J., Forte, T. M., and Anderson, D. W. (1976) Effects of guanidine hydrochloride on human plasma high density lipoproteins, *Biochim. Biophys. Acta 446* (1), 226−239.
34. Silver, E. T., Scraba, D. G., and Ryan, R. O. (1990) Lipid transfer particle-induced transformation of human high density lipoprotein into apolipoprotein A-I-deficient low density particles, *J. Biol. Chem. 265*, 22487−22492.
35. Liang, H. Q., Rye, K. A., and Barter, P. J. (1996) Remodelling of reconstituted high density lipoproteins by lecithin: Cholesterol acyltransferase, *J. Lipid Res. 37*, 1962−1970.
36. Rye, K. A., Hime, N. J., and Barter, P. J. (1997) Evidence that cholesteryl ester transfer protein-mediated reductions in reconstituted high density lipoprotein size involve particle fusion, *J. Biol. Chem. 272*, 3953−3960.
37. Courtney, H. S., Zhang, Y. M., Frank, M. W., and Rock, C. O. (2006) Serum opacity factor, a streptococcal virulence factor that binds to apolipoproteins A-I and A-II and disrupts high-density lipoprotein structure, *J. Biol. Chem. 281*, 5515−5521.
38. Tanford, C. (1980) *The Hydrophobic Effect: Formation of Micelles and Biological Membranes*, pp 57, Wiley-Interscience, New York.
39. Vitello, L. B., and Scanu, A. M. (1976) Studies on human serum high density lipoproteins. Self-association of apolipoprotein A-I in aqueous solutions, *J. Biol. Chem. 251* (4), 1131−1136.
40. Formisano, S., Brewer, H. B., Jr., and Osborne, J. C., Jr. (1978) Effect of pressure and ionic strength on the self-association of apo-A-I from the human high density lipoprotein complex, *J. Biol. Chem. 253* (2), 354−359.
41. Saito, H., Dhanasekaran, P., Nguyen, D., Holvoet, P., Lund-Katz, S., and Phillips, M. C. (2003) Domain structure and lipid interaction in human apolipoproteins A-I and E: A general model, *J. Biol. Chem. 278*, 23227−23232.
42. Saito, H., Dhanasekaran, P., Nguyen, D., Deridder, E., Holvoet, P., Lund-Katz, S., and Phillips, M. C. (2004) α-Helix formation is required for high affinity binding of human apolipoprotein A-I to lipids, *J. Biol. Chem. 279*, 20974−20981.
43. Kunitake, S. T., and Kane, J. P. (1982) Factors affecting the integrity of high density lipoproteins in the ultracentrifuge, *J. Lipid Res. 23*, 936−940.
44. de Beer, M. C., Castellani, L. W., Cai, L., Stromberg, A. J., de Beer, F. C., and van der Westhuyzen, D. R. (2004) ApoA-II modulates the association of HDL with class B scavenger receptors SR-BI and CD36, *J. Lipid Res. 45*, 706−715.
45. de Beer, M. C., van der Westhuyzen, D. R., Whitaker, N. L., Webb, N. R., and de Beer, F. C. (2005) SR-BI-mediated selective lipid uptake segregates apoA-I and apoA-II catabolism, *J. Lipid Res. 46*, 2143−2150.
46. Webb, N. R., Cai, L., Ziemba, K. S., Yu, J., Kindy, M. S., van der Westhuyzen, D. R., and de Beer, F. C. (2002) The fate of HDL particles in vivo after SR-BI-mediated selective lipid uptake, *J. Lipid Res. 43*, 1890−1898.
47. de Beer, M. C., Durbin, D. M., Cai, L., Mirocha, N., Jonas, A., Webb, N. R., de Beer, F. C., and Der Westhuyzen, D. R. (2001) Apolipoprotein A-II modulates the binding and selective lipid uptake of reconstituted high density lipoprotein by scavenger receptor BI, *J. Biol. Chem. 276*, 15832−15839.

BI700496W